

An empirical model for the beams of radio pulsars

Aris Karastergiou¹ & Simon Johnston²

¹ *IRAM, 300 rue de la Piscine, Domaine Universitaire, Saint Martin d’Heres, France.*

² *Australia Telescope National Facility, CSIRO, P.O. Box 76, Epping, NSW 1710, Australia.*

12 November 2018

ABSTRACT

Motivated by recent results on the location of the radio emission in pulsar magnetospheres, we have developed a model which can account for the large diversity found in the average profile shapes of pulsars. At the centre of our model lies the idea that radio emission at a particular frequency arises from a wide range of altitudes above the surface of the star and that it is confined to a region close to the last open field lines. We assert that the radial height range over which emission occurs is responsible for the complex average pulse shapes rather than the transverse (longitudinal) range proposed in most current models. By implementing an abrupt change in the height range to discriminate between young, short-period, highly-energetic pulsars and their older counterparts, we obtain the observed transition between the simple and complex average pulse profiles observed in each group respectively. Monte Carlo simulations are used to demonstrate the match of our model to real observations.

Key words: pulsars:general

1 INTRODUCTION

In this paper, we create an empirical model for the beams of radio pulsars, a model which we believe can account for much of the phenomenology seen in the observations. We use the model to generate a large number of artificial pulsar profiles and statistically compare them to recently acquired, high quality pulsar data. We believe the simplicity of the model to be one of its main strengths, in particular for a better theoretical understanding of the radio emission process.

The integrated profiles of radio pulsars are one of their defining characteristics. Made up from the summation of several thousand single pulses, in the vast majority of cases these integrated profiles are highly stable over decades of observing. It is precisely this profile stability that allows for the determination of highly accurate pulse arrival times leading to the exquisite tests of physics for which pulsar astronomy is renowned (e.g. Kramer et al. 2006).

Each pulsar has its own unique integrated profile consisting of a (usually small) number of Gaussian-shaped components (Kramer et al. 1994), and even a cursory examination of the many hundreds of profiles available in the literature shows that they come in a bewildering variety of forms. This variety owes partly to the shape of the pulsar beam and partly to the geometry of the star and the relative orientation to the observer. Unfortunately, it is very difficult to determine the viewing geometry, and therefore also the true pulsar beam shape. Nevertheless, over the years many different attempts have been made to classify the integrated profiles into groups with well defined characteristics. Two different ideas have emerged, each with their own pros and cons. In the work of Rankin and co-workers (Rankin 1983; Rankin 1993; Mitra & Rankin 2002), emission is recognised as arising from near the magnetic pole of the star (‘core’ emission) and in concentric rings around the pole (‘cone’ emission). This is a natural explanation for symmetric pulse pro-

files and for profiles with an odd number of components. In contrast, Lyne & Manchester (1988) argue that the emission cone is patchy with emission occurring at random locations in the beam convolved with an annular ‘window function’. This more obviously explains the asymmetry seen in many profiles (Han & Manchester 2001).

Unfortunately there exists no sound theoretical basis for the radio emission from pulsars. This makes it difficult to tie down the observed phenomenology of the integrated profiles to any physical understanding of the conditions in the magnetosphere. However, conal structures are predicted by some models (e.g. Ruderman & Sutherland 1975).

We outline in this paper the basic ingredients of an empirical model for the three dimensional location of radio emitting regions in the pulsar magnetosphere. The main purpose of this model is to account for profiles which obey what we consider the current strongest observational constraints with only a small number of free parameters. As we are mostly unable to well determine the true viewing geometry of each observed pulsar, our approach in testing the model is rather a statistical one. In generating large numbers of artificial profiles, we consider to have chosen reasonable parameters for our model when we reproduce a similar range of profile characteristics as in our observed sample.

In the following section we review the important observational results related to integrated pulse profiles. We then outline our model and discuss its parameters. We show how the results from simulations match the observational data, draw some initial conclusions and outline our future work.

2 OBSERVATIONAL BACKGROUND

2.1 Pulsar phenomenology

Pulsar radio emission is thought to arise from the open field lines, with angular radius ρ surrounding the magnetic pole. The pole is inclined by an angle α with respect to the rotation axis. The line of sight traverses the beam; the closest approach of the line of sight to the magnetic axis is the angle β . Under this geometry, the observed pulse width, W , is related to ρ via

$$\sin^2\left(\frac{W}{4}\right) = \frac{\sin^2(\rho/2) - \sin^2(\beta/2)}{\sin\alpha \cdot \sin(\alpha + \beta)} \quad (1)$$

(Gil et al. 1984). For regions close to the magnetic axis and dipolar field lines, ρ is related to the height H above the surface of the star:

$$\rho \sim \sqrt{\frac{9\pi H}{2cP}}, \quad (2)$$

where c is the speed of light and P the pulse period.

In explaining the shape of pulsar profiles, there are several observational lines of evidence which we believe any phenomenological model should reproduce. These are

- **single component profiles:** A large fraction of the observed pulsar profiles consist of a single component. Increased temporal resolution may, in many cases, indicate that the single component consists of several Gaussian components that largely overlap (e.g. Wu et al. 1998).

- **evidence for conal emission:** In the profiles that are not single, symmetry is often present (e.g. PSRs B1133+16 and B0525+21). In such cases the most natural explanation is that the emission originates from a ring centered on the magnetic pole.

- **the period-width relationship:** Rankin has shown good evidence that the profile width, W , depends on the pulsar period, P , as $W \propto P^{-0.5}$. This is an important result and implies (see equation 2) that the height at which a pulsar emits is largely independent of its period (Rankin 1993).

- **the emission height versus pulse longitude:** More than two decades ago, Krishnamohan & Downs (1983) put together an attractive cartoon to explain the properties of the Vela pulsar by proposing that emission components originated from different heights in the magnetosphere at a particular frequency. Rankin (1993) dwells briefly on this idea as an alternative explanation to nested cones. More recently, Gangadhara & Gupta (2001) showed for PSR B0329+54 that the emission heights at a given frequency vary as a function of pulse longitude with high emission heights seen at the edges of profiles and low emission heights in the central parts of the profile. Furthermore, Mitra & Rankin (2002) show that inner cones originate from lower in the magnetosphere than outer cones. The combination of these results is a key result which breaks the long-held assumption that emission at a given frequency arises from a uniform height above the pole.

- **the simplicity of young pulsar profiles:** Johnston & Weisberg (2006) showed that the profiles of a group of young pulsars can be reproduced simply by postulating a single, rather wide, cone of emission located relatively high in the magnetosphere following an earlier idea by Manchester (1996). This is in contrast to older pulsars where complex, multi-component profiles are often observed. Differences between young and old pulsars are not only related to the shape of the profile and the spin-down energy, but also to the increased timing noise seen in young pulsars, as opposed to older pulsars. The transition from one group to the other has not yet been explored in this respect.

Table 1. Profile classification for 283 pulsars

$\log \dot{E}$	Single	Double	Multiple	Total
< 35.0	54%	38%	8%	26
33-35	47%	23%	30%	93
32-33	48%	22%	30%	74
< 32	49%	21%	30%	90
$\log(\tau_c)$				
<5.0	58%	38%	4%	24
5-6.5	47%	23%	30%	98
6.5-7.0	37%	30%	33%	60
>7	55%	16%	29%	101
period [ms]				
<150	61%	39%	0%	18
150-400	46%	23%	31%	106
400-700	51%	19%	30%	82
>700	46%	26%	28%	77

- **that cones are not fully illuminated:** The Lyne & Manchester (1988) model for pulsar beams, which takes into consideration a large amount of observational data available at that time, suggests that the emission within the beam boundary occurs in patches with essentially random locations. Occasionally these sub-beams can form regular patterns such as those seen in drifting sub-pulses (Backer 1973).

- **that complex profiles have complex position angle (PA) swings:** It is very noticeable that many simple conal profiles also have the PA swings expected in the rotating-vector-model (RVM, where the PA is fixed by the plane of curvature of the emitting magnetic field line). On the other hand, complex profiles often show strong deviations from the standard RVM picture. The natural explanation here is that overlapping components at different heights cause a distortion of the observed PA swing (Karastergiou & Johnston 2006).

- **that profiles get wider with decreasing observing frequency:** The so-called radius to frequency mapping (RFM) idea is that lower frequencies are emitted higher in the magnetosphere than higher frequencies which naturally results in wider observed profiles (see equation 2). Thorsett (1991) postulated a width-frequency law which essentially accounts for the fact that pulse widening only really occurs at frequencies below ~ 1 GHz; above this value the pulse width is constant.

2.2 Profile classification

We have recently obtained polarization data on more than 250 pulsars, using an unbiased sample of pulsars in the southern sky strong enough to give high signal to noise profiles in less than 30 minutes at the Parkes radio telescope. Our aim was to establish a new, large database of pulsar profiles observed at multiple frequencies with high temporal resolution (Karastergiou et al. 2005; Karastergiou & Johnston 2006; Johnston et al. 2006). We devised a simple classification scheme by visual inspection of the profiles. The temporal resolution of the profiles was large, with up to 2048 bins per profile. Profiles were classified into ‘single’, ‘double’ and ‘multiple’ component profiles, and then sorted by their spin down energy, \dot{E} , characteristic age, $\tau_c = P/(2\dot{P})$, and period, P . The results are listed in Table 1.

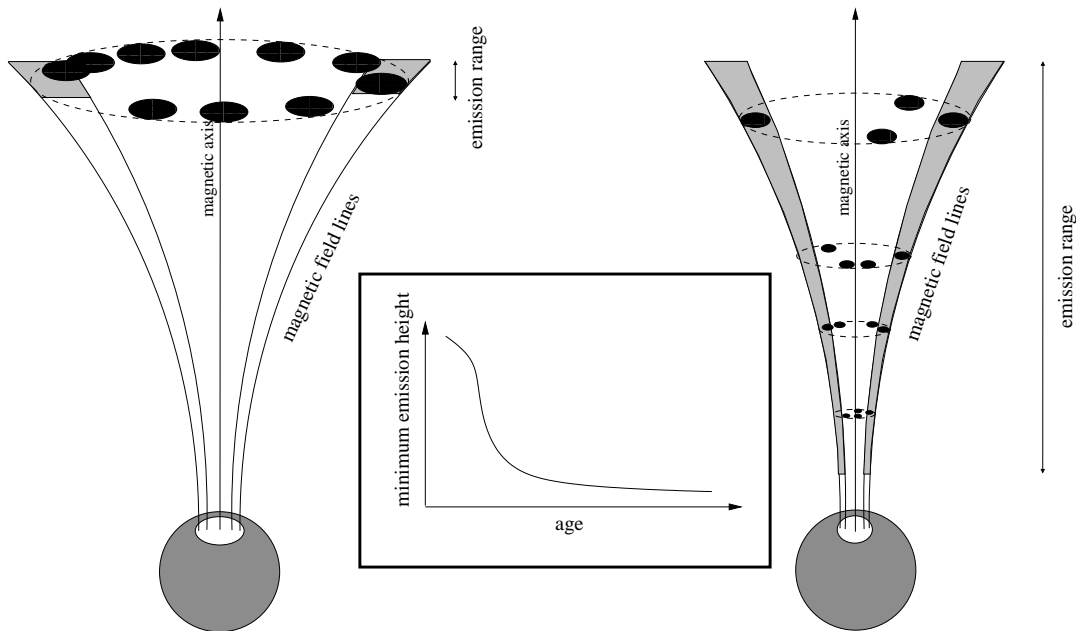


Figure 1. A cartoon of the proposed model. On the left we show the model for young pulsars with emission arising from a patchy conal ring over a narrow range at high altitudes. On the right, the case for older pulsars is shown. Here, the polar cap is smaller and emission at a given frequency arises from close to the surface to a height of ~ 1000 km in a series of discrete patchy rings. The middle panel shows the proposed variation in the minimum emission height with increasing characteristic age, increasing period and decreasing \dot{E}

A priori, it is not clear how the complexity of the pulse profile relates back to physical parameters. The spin down energy determines the power available but the radio luminosity is only a tiny fraction of this power. The pulse period affects the size of the polar cap and light cylinder and should likely be important. The age, on the other hand, is hard to determine with accuracy and may not play a direct role in the energetics.

In Table 1, however, we see a very striking result which is replicated in all three parameters. The young, fast-spinning, highly energetic pulsars **do not** have complex profiles and have roughly a 60:40 split between single and double component profiles. In contrast, the older, slower spinning, less energetic stars do have complex profiles and the split between single, double and multiple component pulsars is roughly 45:25:30. Furthermore, there appears to be a rather abrupt transition where complex profiles are formed at $P \sim 150$ ms, $\tau_c \sim 10^5$ yr and/or $\dot{E} \sim 10^{35}$ ergs $^{-1}$. Above this transition point, the relative fractions stay constant. In the following, when we refer to young pulsars, we mean young/short-period/highly-energetic pulsars below this transition point, as opposed to older, slower and less energetic pulsars. The distinguishing parameter we use in the simulations is the pulse period.

3 A SIMPLE BEAM MODEL

We now attempt to understand the observational evidence and reconcile the nested cone models of Rankin with the patchy models of Lyne & Manchester in a simple way. We postulate a beam model which has the following ingredients:

- radio emission originates from field lines close to the outer edge of the beam, forming an emission cone;
- the conal beam is patchy;

- the maximum altitude of emission, in all pulsars, is set to ~ 1000 km at a frequency of ~ 1 GHz;
- the minimum altitude of emission is large for young pulsars (similar to the maximum altitude) and small (~ 20 km) for older pulsars;
- emission arising from discrete locations within the entire range of emission heights is possible at a given frequency;
- the polarization PA of each patch is tied to the magnetic field line at the centre of that patch.

Figure 1 illustrates the model which naturally reproduces virtually all the observational phenomenology outlined in section 2. In particular, in older pulsars, the large range of allowable heights gives rise to apparent “nested” emission zones resulting in a complex profile.

The limitations we place on the origins of emission within the radio beam immediately pose a question as to the nature of so-called ‘core’ emission in pulsars. In our approach here, central components, which are often seen to have special properties (for example a steeper spectrum), are tangential cuts of emission patches which are deeper in the beam structure and therefore naturally closer to the magnetic axis. As these components arise from lower altitudes, they are naturally flanked by components originating from higher up in the magnetosphere. In a similar geometrical approach, Sieber (1997) attempted an explanation of ‘core’ components within the framework of the nested cone model.

In the following, we assume that all emitting patches within the beam have the same peak brightness. We attribute profiles with components of different strengths to the specific line-of-sight cut and overlapping components (see Figure 2). Observationally, this seems reasonable, as it is rare that pulsar profiles contain either very large or very tiny amplitude components. At the same time, pulsars are not standard candles, but the reason for a given pulsar’s

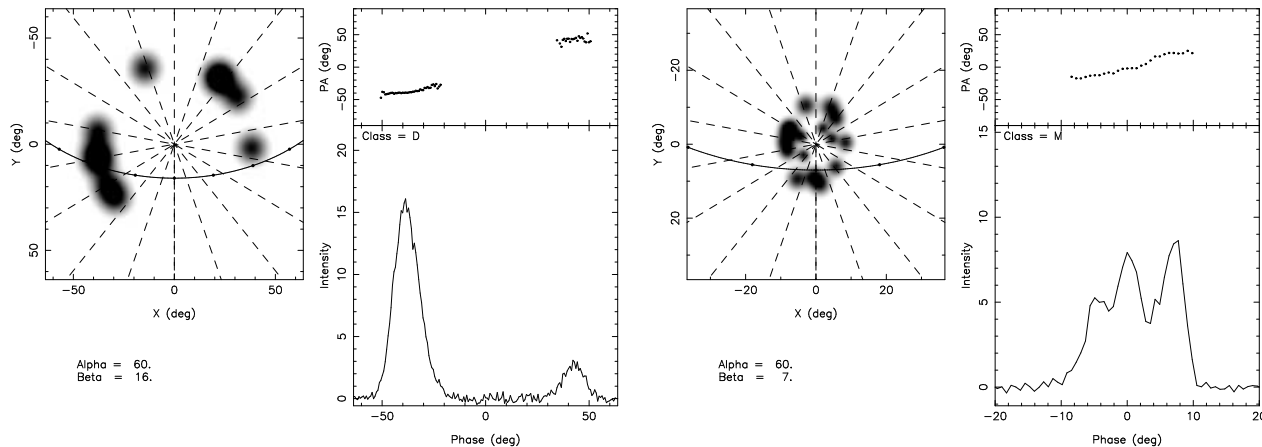


Figure 2. Artificial beams and profiles generated for a young pulsar with period of 100 ms (left) and an older pulsar with period of 1000 ms (right). The beam is shown from above the magnetic pole, and the line of sight is also depicted. Note the narrower patches originating from lower altitudes in the beam depicted on the right. Above the pulse profile, we show the polarization PA obtained according to the model. Deviations from the simple RVM are caused by overlapping patches. Longitude zero depicts the magnetic pole crossing.

luminosity is not known, nor does there appear to be any strong correlation between luminosity and any other pulsar parameter. Also, as we are postulating patches of emission, we create inhomogeneity in the brightness of the pulsar beam. There is no way that this brightness distribution can be decomposed uniquely into patches of variable brightness.

Out of the model ingredients, which determine the three-dimensional beam, some are well constrained by observations and can be fixed to certain values, while others are unconstrained and explored using numerical simulations. For the minimum and maximum emission heights, and the size of the emitting patches, there are a number of assumptions which guide us to the values used in our simulations, which we explain in more detail in the following section. On the other hand, we have no previous constraints on the discrete emitting heights and patches of emission per height, and are forced to explore a large area of the parameter space to appreciate their role.

3.1 Constraints to the model

As mentioned earlier, Rankin (1993) shows convincing evidence that the maximum emission height is independent of the pulsar period. Typical maximum emission heights from the literature range from ~ 10 to ~ 1000 km above the stellar surface (Blaskiewicz et al. 1991, Mitra & Li 2004). The model presented here retains a constant maximum height for pulsars of all periods. For our simulations, we fixed the maximum emission height at 1000 km at a frequency of 1 GHz.

For the minimum height, we consider two populations distinguished by the period P . In order to reproduce the values shown in Table 1 we set the minimum height to be very near the maximum height in short period pulsars ($P < 0.15$ s). For longer periods, the higher complexity in the pulse profiles leads us to set the minimum height much further down in the magnetosphere. In our simulations, we choose a minimum height just above the stellar surface for all pulsars with $P > 0.15$ s. We set this abrupt transition in accordance with the profile classification in section 2.2.

In this context, it is interesting to examine the consequences of setting the emission height range to be a constant fraction of the neutron star light cylinder radius. For example, a pulsar with 0.1 s

period, has a light cylinder radius of 4800 km. If radio emission occurred over a height range spanning 2% of the light cylinder radius, this corresponds to ~ 100 km and so the allowable emission heights would range from 900 to 1000 km. For an older, 1 s period pulsar, the light cylinder grows to 48000 km, 2% now corresponds to ~ 1000 km and the entire range from the surface of the star to the maximum emission height is now allowed. Although this line of thinking is appealing, it presents difficulties in explaining the abrupt change in the profile classification seen in Table 1 and discussed earlier.

The width of a patch of emission at a given height is a key parameter for the model. We use two sources to derive this. First, Johnston & Weisberg (2006) estimate that the conal width, Δs in young pulsars is about 20% of the total width available. Secondly, Mitra & Rankin (2002) measure component widths as a function of emission height in a variety of double component pulsars. We use their equation to assign a patch width based on emission height

$$w_p = 2.45^\circ \Delta s \sqrt{\frac{H}{10 \cdot P}}, \quad (3)$$

with $\Delta s = 0.2$ and H expressed in km.

4 RESULTS

A large number of numerical simulations have been performed to constrain the remaining free parameters, namely the active altitudes and the patches per emission height. As concerns the number of heights and patches, we have explored the parameter space ranging from 1 to 10 discrete heights and 1 to 10 patches per height. We have no a priori knowledge on the location of these heights and patches and pick their positions randomly in our simulations. These consist of “creating” patchy beams according to the model. Each beam is then systematically cut with 300 different lines of sight, spanning a reasonable range of α and β . This results in a “clean” profile for each line of sight, to which an amount of Gaussian noise is applied before passing it through an automated classification process to determine whether the generated profile is single, double or multiple. This process takes the local maxima before the addition of noise and assesses them after noise addition to determine whether

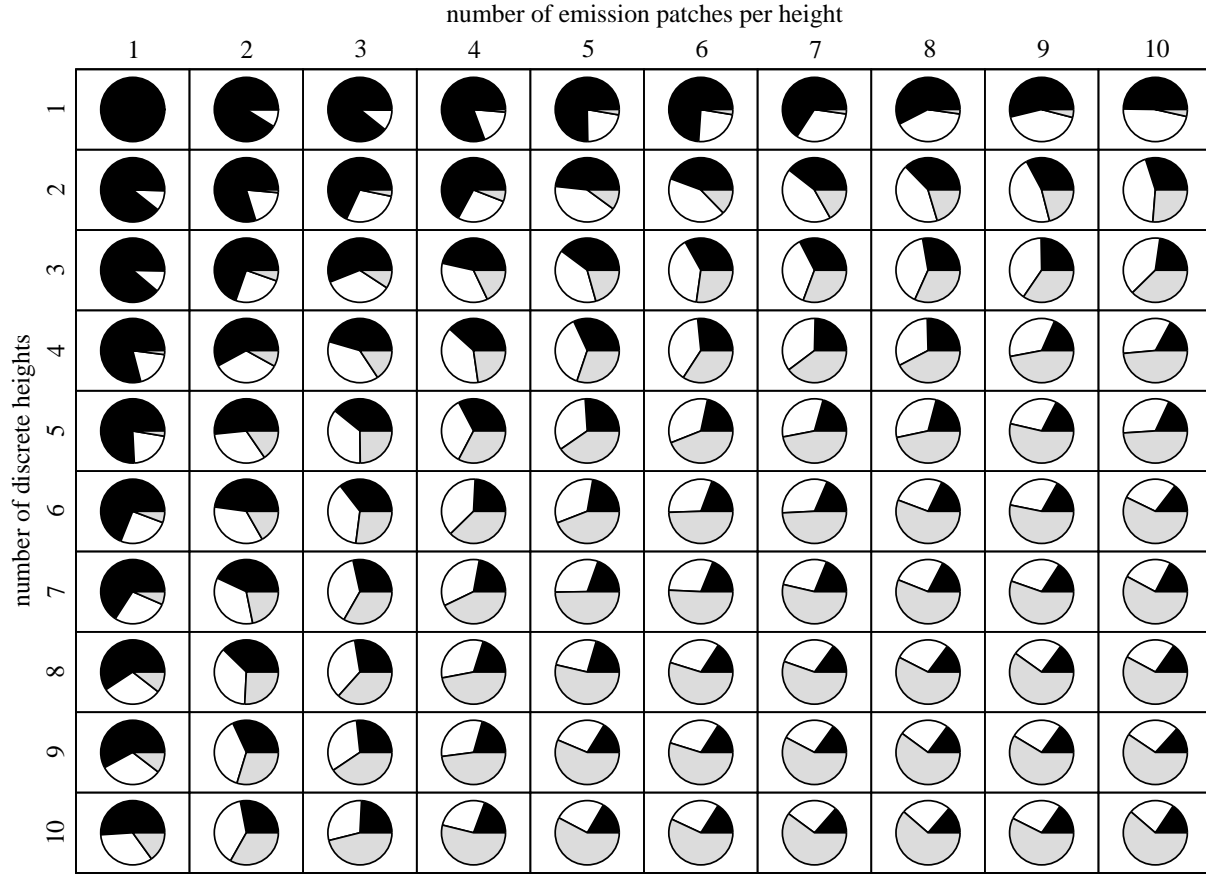


Figure 3. The results of a numerical simulation of 10^5 average profiles for a pulse period of 0.3 s. 10^3 artificial profiles are generated for each combination of number of heights (y-axis) and number of patches (x-axis). The pie charts show the fraction of generated profiles which are single- (black), double- (white) and multiple-component (grey).

their separation in the intensity-time diagram is adequate compared to the noise. Empirical fine tuning was applied to match the results with our own visual interpretation of the profiles. The process was repeated a large number of times due to the randomness in the discrete heights and location of the patches. Following this procedure, we check what fraction of the artificially generated profiles are single, double or multiple for a given combination of emitting heights and patches per height. This test also results in a predicted beaming fraction, that is the fraction of pulsars we would expect to detect given a certain beam configuration.

In a second test, we create large sets of 1000 average profiles per combination of emitting heights and patches per height, using a randomly computed viewing geometry per profile. We chose from a subset of α and β which guarantees that the line of sight intersects the cone of emission. Figure 3 shows an example of such a simulation of $10 \times 10 \times 1000$ beams. The plot demonstrates clearly how a single emitting altitude (top line) can not account for a substantial fraction of multiple component profiles. It also demonstrates how, as the total number of heights and components grows, the fraction of single profiles becomes small.

4.1 Young, short-period pulsars

The observational data suggests that over 50% of the profiles in this category comprise of a single component. The rest are almost all symmetrical doubles and only a very small number of multiple component profiles exist (see Table 1). Evidence that emission from such objects generally arises from high altitudes has been presented in Johnston & Weisberg (2006) and we therefore limit our range of emission heights from 950 to 1000 km. However, the fraction of single profiles also forces the total number of patches to be rather small, so that the line of sight will intersect only one patch on half of the observed cases. We find the best value to be 10 patches in total, at a single emission height. Our simulations also provide a rough estimate of the beaming fraction. For this group, we find the beaming fraction to be around 30%. An example of a simulated artificial beam and profile from this group can be seen in the left hand panel of Figure 2.

4.2 Older, slower pulsars

In contrast to young pulsars, this group shows large diversity in the shapes of the observed profiles. In particular there is a large fraction of multiple component profiles (see Table 1) but this fraction does not appear to change either with \dot{E} , τ_{avc} or P . In our model, we attribute this diversity to the wide range of active emission heights at a given frequency.

We note that as a pulsar's period increases, because the maxi-

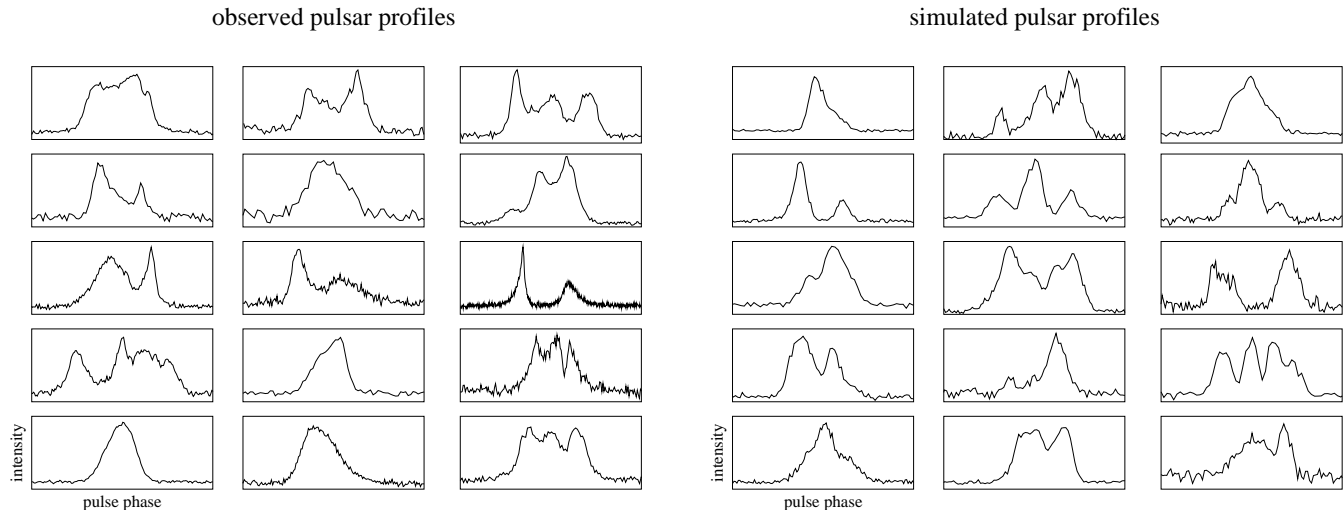


Figure 4. The left panel shows fifteen profiles randomly selected from our database of pulsar polarization data obtained at 1.4 GHz with the Parkes radio telescope. These show the usual variety of phenomenology such as multiple components and components of various width, amplitude and shape. On the right are fifteen simulated profiles according to our model. Although a direct one-to-one comparison is not our intention here, the same sort of profile variety as exists in the real data is clearly reproduced.

num emission height is constant, both ρ and W must decrease (see equations 1 and 2). At the same time individual component widths decrease in a similar fashion according to equation 3. This naturally forces pulse profiles to be very similar looking (although with different widths) for all slower pulsars, similar to the statistics from Table 1. We find that we can reproduce these statistics as long as we permit at least 3 active heights, and a number of active patches per height roughly ranging from 2 to 7, depending on the number of heights. We obtain the best match to the observations when the total number of patches is $\sim 16 \pm 4$ (example, for 4 active heights, 3-5 active patches per height). Pulsars with periods of 0.2 s have a beaming fraction of around $\sim 18\%$, whereas only $\sim 5\%$ of 2 s pulsars would be detected, similar to results obtained from population studies (Tauris & Manchester 1998). An example of a simulated artificial beam and profile from this group can be seen in the right hand panel of Figure 2.

A visual inspection of the artificial profiles yields a strong affirmation of a hollow cone of emission, with many symmetrical double profiles. A number of instances of characteristic triple profiles, with a strong central component and weaker outrider components also randomly arise. We are also encouraged by the fact that our simulations never result in profiles with an unacceptably high number of distinct components, with a maximum of ~ 5 similar to the observed population. To illustrate these points, Figure 4 shows a comparison between randomly selected, artificial pulse profiles and real observational data.

4.3 Radius-to-frequency mapping - RFM

Up to this point, we have drawn results from simulations at a single observing frequency near 1 GHz. However, we can also add RFM to our model, following ideas from Rankin & Mitra (2002). They interpreted the earlier work of Thorsett (1991) and showed that the height of emission has a functional form

$$H_\nu = K \cdot \nu^{-2/3} + H_0, \quad (4)$$

with K and H_0 picked to ensure little evolution of the profile width above ~ 1 GHz. In the standard model, H_ν is constant across the

pulse. In our model, however, we compute H_ν for every created patch. Figure 5 shows three examples obtained for our implementation of RFM. The impact angle β changes from left to right, from -6° to 6° to 12° . The profile width changes with frequency according to equation 4 combined with equation 2. Note the apparent change of the component amplitude ratios as a function of frequency. This is especially striking in the second and third examples where a central component at low frequencies quickly disappears at high frequencies. This apparent spectral index change between components is then purely geometric in this model as originally suggested by Sieber (1997). In the first panel of Figure 5, the pulse profile becomes very weak above 4 GHz as the beam becomes narrower and is no longer directed towards the line-of-sight.

4.4 The polarization position angle

In this paper we do not intend to present a detailed treatment of the polarization of average pulsar profiles in the context of our model. However, it is useful to look at the consequences of our model, particularly on the PA swing. In particular, we note the disruption of smooth average PA swings in complex profiles and believe our model can also reproduce this. In the model, we tie the PA of each patch to the magnetic field line of the centre of the patch. In complex profiles, where there may be several overlapping patches, this causes significant distortion of the (geometrical) PA angle swing which is qualitatively similar to real data (see Figure 2).

5 SUMMARY AND FUTURE WORK

We have developed a beam model for the radio emission from pulsars, where emission is generated at more than one discrete height at a given frequency. The emission occurs in a ring close to the last open field lines. Emission from a given ring is patchy. Following extensive numerical simulations, Table 2 shows the parameters from the model which best reproduce the features of the observational data. The model yields

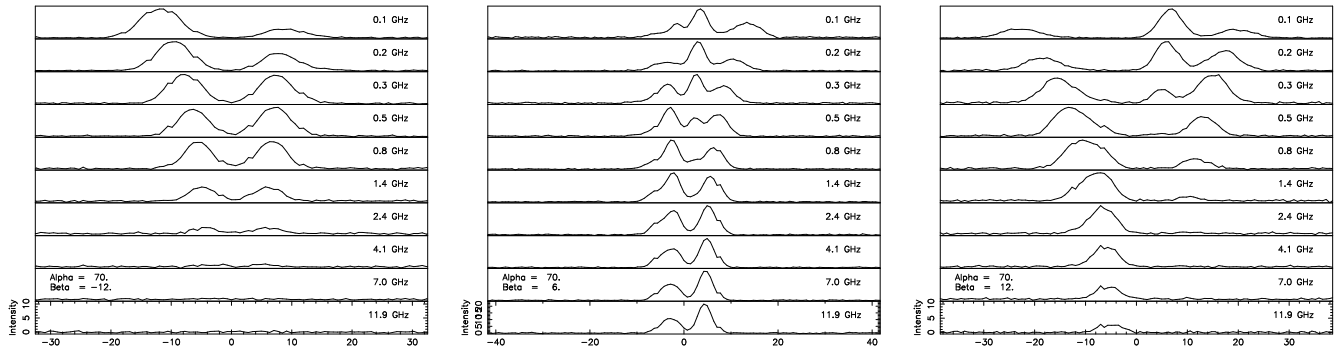


Figure 5. Three examples of simulated profiles at 10 different observing frequencies. As a consequence of equation 4, the pulse profile becomes narrower at higher observing frequencies. In all cases there are substantial profile shape changes between low and high frequencies. The middle and right hand panels show that the smaller, lower altitude patches seen towards the centre of the profile have an apparently steeper spectral index than the outrider components, similar to what is observed in the known pulsars. The panel on the left demonstrates how geometry hampers high frequency observations, as the line of sight no longer intersects the pulsar beam.

Table 2. Model Parameters

Pulsar group	Young	Old
Maximum height:	1000 km	1000 km
Minimum height:	950 km	20 km
Distinct emission heights:	1	> 3
Active patches per height:	10	2 ... 7
Total number of patches:	10 ± 1	16 ± 4

- the simple profiles of young, energetic pulsars as opposed to more complex profiles of the older population;
- a wide variety of simulated profiles which closely resembles the observations;
- an explanation for the number of single-component profiles through the patchiness of the ring structure at a given height;
- a complex PA angle profile for complex profiles, as in the observed data;
- RFM behaviour consistent with the observations;
- beaming fractions as a function of period which are consistent with other studies.

From a theoretical point of view, the idea that emission arises only from near the last open field lines is appealing. Our model requires a successful theory that gives rise to emission at many heights at a particular frequency rather than emission at many locations across the polar gap. As the emission properties are tied somehow to the plasma conditions, one could postulate a varying plasma density along the vertical extent of the emission tube as a possible explanation for multiple emission heights.

We recognise that there are several observational differences between the outer and inner parts of pulsar profiles. In particular they may have different drift rates and certainly have different modulation properties. Generally this has been assumed to be caused by different emission properties between the outer and inner magnetic field lines. However, in the absence of any physical model, this could equally likely be caused by differences between higher and lower altitudes as would be the case in our model. A lot of important work is being carried out presently on the drifting properties of individual pulses (e.g. Weltevrede et al. 2006, 2007), some of it indicating close relationships between the drift rates of the various rings that are postulated to form the beam (Bhattacharyya et al.

2007), although a clear picture has yet to emerge concerning how these drift patterns ultimately form an average pulse profile.

Currently our model is designed to reproduce the total intensity profiles and we therefore only lightly touch on polarization aspects of pulsar emission. Much exciting work has also been done in this area recently and we plan to incorporate polarization into the next iteration of the model.

In summary we have produced a simple beam model of pulsar radio emission, which can generate average pulse profiles in accordance with the most current observational constraints. Its main features are that it postulates emission over a wide range of emission heights rather than over a wide range of beam longitudes as in previous models and that it largely replicates the observational data.

ACKNOWLEDGMENTS

We thank Don Melrose and Steve Ord for valuable discussions during the writing of this paper and Michael Kramer for parts of the simulations code. AK particularly thanks Don Melrose at the University of Sydney for his hospitality and acknowledges financial support from the 6th European Community Framework programme through a Marie Curie, Intra-European Fellowship. The Australia Telescope is funded by the Commonwealth of Australia for operation as a National Facility managed by the CSIRO.

REFERENCES

- Backer D. C., 1973, ApJ, 182, 245
 Bhattacharyya B., Gupta Y., Gil J., Sendyk M., 2007, MNRAS, 377, L10
 Blaskiewicz M., Cordes J. M., Wasserman I., 1991, ApJ, 370, 643
 Gangadhara R. T., Gupta Y., 2001, ApJ, 555, 31
 Gil J. A., Gronkowski P., Rudnicki W., 1984, A&A, 132, 312
 Han J. L., Manchester R. N., 2001, MNRAS, 320, L35
 Johnston S., Karastergiou A., Willett K., 2006, MNRAS, 369, 1916
 Johnston S., Weisberg J. M., 2006, MNRAS, 368, 1856
 Karastergiou A., Johnston S., 2006, MNRAS, 365, 353
 Karastergiou A., Johnston S., Manchester R. N., 2005, MNRAS, 359, 481

- Kramer M., Stairs I. H., Manchester R. N., McLaughlin M. A., Lyne A. G., Ferdman R. D., Burgay M., Lorimer D. R., Possenti A., D'Amico N., Sarkissian J. M., Hobbs G. B., Reynolds J. E., Freire P. C. C., Camilo F., 2006, *Science*, 314, 97
- Kramer M., Wielebinski R., Jessner A., Gil J. A., Seiradakis J. H., 1994, *A&AS*, 107, 515
- Krishnamohan S., Downs G. S., 1983, *ApJ*, 265, 372
- Lyne A. G., Manchester R. N., 1988, *MNRAS*, 234, 477
- Manchester R. N., Wide beams from young pulsars (or one pole for all). pp 193–196
- Mitra D., Li X. H., 2004, *A&A*, 421, 215
- Mitra D., Rankin J. M., 2002, *ApJ*, pp 322–336
- Rankin J. M., 1983, *ApJ*, 274, 333
- Rankin J. M., 1993, *ApJ*, 405, 285
- Ruderman M. A., Sutherland P. G., 1975, *ApJ*, 196, 51
- Sieber W., 1997, *A&A*, 321, 519
- Tauris T. M., Manchester R. N., 1998, *MNRAS*, 298, 625
- Thorsett S. E., 1991, *ApJ*, 377, 263
- Weltevrede P., Edwards R. T., Stappers B. W., 2006, *A&A*, 445, 243
- Weltevrede P., Stappers B. W., Edwards R. T., 2007, *A&A*, 469, 607
- Wu X., Gao X., Rankin J. M., Xu W., Malofeev V. M., 1998, *Astron. J.*, 116, 1984